Crop rotation combined with controlled-release fertilizer promoted the utinization of the reclaimed land along Yanze River through improving soil fertility and nutrients use efficiency

Xuebin Xu[1], Fei Ma[1], Jianmin Zhou[1], and Changwen Du[1]

[1]State Key Laboratory of Soil and Sustainable Agriculture

June 13, 2022

Abstract

Although fertilization of controlled-release fertilizer (CRF) and crop rotation have been shown the contribution to improving yield, nutrient use efficiency, and soil fertility, their interactions on the quality of relcalimed land remains unclear. Hence, a field experiment was conducted in a reclaimed land along Yangze River to investigate their interactions. Results indicated that application of bulk blending urea (BBU) of conventional urea and controlled-release urea (CRU) with appropriate dosage and frequency increased the rice yield and nitrogen agronomic efficiency (NAE). Crop rotation also improved the rice yield and NAE through enhancing the retention capability of fertility. Crop rotation combined with fertilization significantly increased the soil pH, organic carbon (SOC), total N (TN), and permanganate oxidizes carbon (POXC). The rice-green manure (RG) rotation improved soil pH and TN most, and the rice-rape (RR) rotation improved SOC most. Fertilization of conventional urea and BBU both significantly increased the labile SOC functional groups and reduced the the stabled SOC functional groups under RG rotation. Under RR rotation, however, only fertilization of conventional urea increased the labile SOC functional groups and reduced the the stabled SOC functional groups. The rice-wheat (RW) rotation showed no significant effects on the changes in soil organic functional groups. The changes in soil properties had significant effects on improving rice yield or NAE under RG and RR rotations instead of RW rotation. The findings suggested that BBU combined with crop rotations could make good use of reclaimed land through improved nutrient use efficiency and soil fertility.

1. Introduction

An extreme imbalance between the arable area and population exists in China which has 20 percent of the world's population but only 7 percent of the world's arable land (Piao et al., 2010). With the rapid socio-economic development, more and more arable lands are occupied by industry and urban construction, resulting in a sharp decrease in the arable land (Li, Liu, & Yang, 2018). So far, under the pressures of food safety and the arable land red line continued to increase, enclose tideland for cultivation are widely used to increase the arable land and ensure the adequate production of grain (L. Chen et al., 2020; Li et al., 2018; J. Zhao et al., 2020). However, the soil in reclamation land usually is seriously impoverished which mainly manifests as salination, soil nutrient deficiency, extremely low organic matter content , etc. The high fertility of the soil is the basis for maintaining a high yield of crops (Stewart, Pierzynski, Middendorf, & Prasad, 2020). Therefore, it is necessary to take a series of measures to improve soil fertility and reduce the risk of crop failure for reclamation land.

Application of chemical fertilizer is the most common way to improve the permeability of soil structure and provide abundant nutrients for crops to maintain grain production (Huang et al., 2019). However, traditional fertilizers, especially nitrogen (N) fertilizer, are extremely water-soluble and are easily transferred and transformed between the soil-water-atmosphere environment according to the soil structure and property (Fu, Duan, Zhu, Gao, & Xu, 2021). The soil in reclamation land is mainly sandy loam with lower fertility holding capacity, resulting in the inefficient of traditional fertilizers. Moreover, unreasonable application of fertilizer has the risk of the non-point source due to the losses of reactive N to the surface water, groundwater, and atmosphere (J. Chen et al., 2018; Liu et al., 2021; Yang & Lin, 2019). Coated controlled-release fertilizer (CRF) is prepared by coating the conventional fertilizer with a hydrophobic material and it has the characteristics of controlled nutrient release (Shen, Du, Zhou, & Ma, 2017). Nutrients in coated CRF are regulable to supply for crop growth according to the requirement by adjusting the amount and property of coating (Tomaszewska & Jarosiewicz, 2002). The improvements of the water efficiency, N-use efficiency, and grain yield of maize by application of controlled-release urea (CRU) combined with subsoiling had been confirmed by Hu et al. (2013) in northern China. Guo et al. (2019) also demonstrated that the CRU treatment decreased the annual NH_3 volatilization, CH_4 emission by 64.8%, 19.7%, and 35.2%, respectively in a paddy field. Gao et al. (2021) showed that the CRF treatment significantly improved soil aggregate characteristics and increased humic acid, fulvic acid, lignin-like molecules, and protein-like molecules content. Therefore, CRF has the potential to improve fertilizer use efficiency, soil structure, and soil fertility and relieve a series of environmental problems, such as eutrophication and groundwater pollution. However, the effects of CRF on the improvement of soil fertility and the change in soil organic and mineral components in the soil from reclamation land are few studied.

Crop rotation has been applied for millennia across China which mainly includes the maize-wheat rotation, peanut-wheat rotation, rice-rape rotation, rice-wheat rotation, and rice-green manure rotation (Zeng et al., 2016). As an environmentally friendly strategy, crop rotation can adequately control nutrients, water, weeds, pests, and diseases, as well as maintain soil structure and fertility which increases the productivity of the land (Bender, Wagg, & van der Heijden, 2016; German, Thompson, & Benton, 2017). For example, Ghosh et al. (2020) indicated that replacing wheat with chickpea in the rice-wheat rotation increased grain yield by 5-8%. A previous study also suggested that the adoption of 2- and 4-year of crop rotations in rain-fed environments could result in high yield compared with continuous cropping (Sindelar, Schmer, Jin, Wienhold, & Varvel, 2016). Malobane, Nciizah, Mudau, and Wakindiki (2020) indicated that the sweet sorghum-grazing vetch-sweet sorghum rotation increased ammonium (NH_4^+-N) and nitrate (NO_3^--N) by 3.42% to 5.98%, respectively. A 9-year corn-wheat-corn-wheat-corn-wheat-alfalfa-alfalfa-alfalfa (*Lotuscorniculatus* L.) rotation indicated that rotation had positive effects on soil organic carbon (SOC), total nitrogen (TN), and soil microbial biomass C, N, and activity (Giacometti et al., 2021). Recently, a meta-analysis across China had demonstrated that crop rotation increased yields by 20% compared to continuous monoculture and the improvement performed better in coarse or medium soil texture and medium level of initial SOC and at low N fertilization rate (J. Zhao et al., 2020). Even so, the impacts of the combination of crop rotation and CRF application on grain yield, soil fertility, and changes in soil organic and mineral components remain unclear, especially in barren soil.

A field trial of three types of crop rotation (rice-green manure, rice-rape, and rice-wheat) combined with different N fertilizer treatments was conducted in a reclamation land. The types of N fertilizer included conventional urea and bulk blending urea (BBU) of conventional urea and CRU. Soil organic and mineral components were characterized by Fourier transform infrared photoacoustic spectroscopy (FTIR-PAS) and mid-infrared attenuated total reflection spectroscopy (FTIR-ATR). The main objective of this study was to investigate the influences of fertilization, crop rotation, and their interaction on rice grain yield, dynamics of soil inorganic N and plant N uptake, soil properties, and soil organic and mineral components.

2. Materials and methods

2.1. Experiment site and design

The field experiment was conducted in a reclamation land in Zhangjiagang city, Jiangsu province (31°57'N, 120deg46'E, Fig. 1). The soil is composed of alluvium from the Yangtze River and classified as Fluvo-aquic according to the Chinese Soil Taxonomy (Gong et al., 2001). The basic soil chemical properties are as follows: pH (H_2O) 8.00+-0.30; SOC 3.86+-1.35 g kg^{-1}; TN 0.41+-0.16 g kg^{-1}; NH_4^+-N 1.36+-0.34 mg kg^{-1}; NO_3^--N 11.58+-5.37 mg kg^{-1}; available phosphorus (AP) 20.57+-12.67 mg kg^{-1}; and available potassium (AK) 7.34+-1.95 mg kg^{-1}.

A plot design with replicates was adopted with 60 m x 35 m (Fig. 1). Rice-green manure (RG), rice-rape (RR), and rice-wheat (RW) rotations were included. Five fertilization treatments were set as follow: without N fertilizer (WN), farmer's conventional urea fertilizing practice with a thrice-split application (CU), single-dose application of BBU with the conventional amount of N (CB1), twice-split application of BBU with the conventional amount of N (CB2), single-dose application of BBU with 20% reduction of N (RB1), and twice-split application of BBU with 20% reduction of N (RB2). The BBU consisted of 75% CRU and 25% conventional urea. The CRU coated with 10% waterborne polyacrylate was purchased from Jiangsu Issas New Fertilizer Engineering & Technology Co., Ltd., China and had an N content of 42% and an N release longevity of 3 months. The farmer's conventional N application rates are 300 and 270 kg N ha^{-1} for rice and wheat, respectively. There was no fertilization during the rape oil and green manure seasons. Superphosphate, potassium chloride, zinc sulfate, and silicon fertilizer were incorporated into the 10-15 cm soil layer for all treatments at rates of 75 kg $P_2O_5 ha^{-1}$, 120 kg K_2O ha^{-1}, 3 kg Zn ha^{-1}, and 0.8 kg SiO_2 ha^{-1} as basal fertilizers in rice and wheat seasons.

2.2. Crop culture and management

Two rice seasons and one crop rotation season were conducted from June 2019 to November 2020. The field had always been cropped with rice-wheat rotation before the experiment. The paddy rice (*Oryza sativa* L.) with the variety of "Nanjing 46" was planted on June 14, 2019, and harvested on November 7, 2019, for the first season (Rice2019), and on June 13, 2020, and harvested on November 17, 2020, for the second season (Rice2020). The winter wheat (*Triticum aestivum* L.) with the variety of "Yangmai 13" was seeded on November 17, 2019, and harvested on May 22 in 2020 (Wheat). The oilseed rape (*Brassica napus* L.) with the variety of "Huayouza No.8" and the green manure of Chinese milkvetch (*Astragalus sinicus* L.) with the variety of "Zhezi No.5" were seeded at the same time as wheat. Straws of rice and wheat were turned over after grain harvesting by a rotary cultivator. Shoots of oilseed rape and Chinese milkvetch were also turned over after maturing. Crops were planted by a planter with the conventional plant density. The base fertilizer was incorporated into the 10-15 cm soil layer before planting and the topdressing fertilizer was broadcasted artificially. Conventional weeding, irrigation, and UAV plant protection were carried out to maintain crop growth.

2.3. Sampling and chemical analyses

Soil samples were collected from each plot before the experiment and after the rice had been harvested to analyze the basic soil properties including pH, SOC, TN, NH_4^+-N, NO_3^--N, AP, AK, permanganate oxidizes carbon (POXC), and other available medium and trace elements. Soil samples were collected for determining NH_4^+-N and NO_3^--N contents at the seeding, tillering, elongation, earing, flowering, and maturation stages, respectively. Quadruplicate soil samples from a depth of 0-20 cm for each plot were collected and mixed thoroughly. The soil samples were air-dried at room temperature and then sieved to < 2 mm and/or < 0.15 mm after removing the residues and plant roots. Soil pH was measured with a pH meter (PH-21, Sartorius, Goettingen, Germany) in a 1:2.5 mass: volume soil/water suspension (Thomas, 1996). SOC content was determined using the potassium dichromatic oxidation titration method (Walkley & Black, 1934). TN content was determined using the Kjeldahl method (Pansu & Gautheyrou, 2006). AP was extracted with sodium bicarbonate solution and then was measured by the molybdenum antimony blue colorimetric method (Olsen, 1954). AK was extracted with 1 N ammonium acetate and then was determined by flame spectrometry (Jackson, 1958). POXC was measured using the colorimetric method after oxidating by 0.02 M $KMnO_4$ (Blair, Lefroy, & Lisle, 1995). Available medium and trace elements were extracted with DTPA-$CaCl_2$-TEA solution and then were measured using an ICP-OES (ICAP7000, ThermoFisher, USA) (Jackson, 1958). Soil NH_4^+-N and NO_3^--N were extracted with 2 M KCl and then were measured using a flow analyzer (San^{++}System, SAKLAR, Netherlands). The shoot and/or grain of rice and wheat were also collected at seeding, tillering, elongation, earing, flowering, and maturation stages, respectively. The oven-dried and ground shoot and grain were digested with sulfuric acid-hydrogen peroxide, and the N content was determined by the Kjeldahl method. The grain yield and the grain moisture were measured during harvesting. Grain yield was adjusted to standard moisture of 15% for rice and 12% for wheat. The

N agronomic efficiency (NAE, kg kg^{-1} N) was calculated as follow:

$$\mathrm{NAE} = \frac{Y_N - Y_0}{F_N} \# (\; AUTONUM \quad \backslash * \; Arabic \;)$$

where Y_0 and Y_N (kg ha^{-1}) are the dry grain yields without N fertilizer and with N treatments respectively, F_N (kg N ha^{-1}) is the N fertilization rate.

2.4. Spectral acquisitions

Soil FTIR-PAS spectra were measured using an FTIR spectrometer (Nicolet 6700, ThermoFisher, USA), equipped with an MTEC model 300 PA accessory. A nitrogen purge was continuously done in the optical system to eliminate the interferences from CO_2 and water vapor. Approximately 5 g soil samples were placed in the photoacoustic cell and the dry helium was then purged into the cell for 10 s. The spectrum of the reference black carbon was used as background to correct the soil spectra. Each spectrum between the wavenumbers of 4000 and 650 cm^{-1} with a resolution of 8 cm^{-1} was finally recorded by averaging 32 successive scans under moving mirror velocity of 0.32 cm s^{-1}.

Soil FTIR-ATR spectra were acquired using an attenuated total reflectance infrared spectrophotometer (Agilent 4300, Agilent Technologies Inc., USA). Approximately 2 g soil samples were placed on the FTIR-ATR crystal and then were compressed for measuring. Each spectrum was finally recorded by averaging 64 successive scans between the wavenumbers of 4000 and 650 cm^{-1} with a resolution of 0.466 cm^{-1}. A background spectrum of air was measured to correct the soil spectra before sample screening.

2.5. Statistical analyses

All soil spectra were smoothed and normalized before spectral analysis in MATLAB R2020b (The Math Works, Natick, USA). A one-way analysis of variance (ANOVA) was used to analyze the effects of various treatments on grain yield, NAE, changes in soil properties, soil NH_4^+-N and NO_3^--N contents, and plant N content. Differences between treatments were determined by comparing their means using the least significant difference (LSD) at the 0.05 probability level. A two-way ANOVA was applied to evaluate the main and interactive effects of crop rotation and fertilization on grain yield, NAE, changes in soil properties, soil NH_4^+-N and NO_3^--N contents, and plant N content. A pairwise samples test was conducted to compare the significant changes in soil properties and characteristic spectral bands after various treatments. Principal component analysis (PCA) was performed to illustrate the internal structure of spectra. A two-way permutational multivariate analysis of variance (PERMANOVA) was applied to evaluate the effect of crop rotation, fertilization, and their interaction on the changes in spectral structures. Regressions between spectral data and SOC, TN, and POXC were built by the partial least squares regression (PLSR) model. The five-fold cross-validation was performed to obtain the optimal number of latent variables in the PLSR model. The variable importance in projections of spectral bands in the PLSR model was used for identifying the great changes in molecular structure for soil organic matter and TN. Structural equation modeling (SEM) was applied to determine the direct and indirect effects of selected variables on grain yield and NAE based on known correlations. The chi-square,P -value, root-mean-square error of approximation (RMSEA), and good fit index (GFI) were used to evaluate the model fitness. All data processing, statistical analysis, and visualization were implemented in R 4.1.0 software (R Development Core Team, 2018).

3. Results

3.1. Grain yield and

nitrogen agronomic efficiency

Under the RG rotation, RG-CB1 and RG-CB2 treatments only increased inappreciable grain yields in both Rice2019 and Rice2020 seasons compared with RG-CU (Fig. 2a). RG-RB1 treatment decreased the grain yields in both Rice2019 and Rice2020 seasons, while the RG-RB2 treatment increased the grain yield in the Rice2019 season. Under the RR rotation, RR-CB2 treatment significantly increased the grain yield in the

Rice2019 season compared with RR-CU. Both RR-RB1 and RR-RB2 treatments had significantly lower grain yields than RR-CU in both Rice2019 and Rice2020 seasons. Under the RW rotation, RW-CB2 treatment showed significantly highest rice grain yield in Rice2019 season and wheat grain yield in Wheat season. Grain yield was significantly affected by fertilization in the Rice2020 season (Table S1, supplementary materials). Crop rotation and the interaction between crop rotation and fertilization had no significant effects on grain yield.

RG-RB2 and RR-RB2 treatments had the highest NAE in the Rice2019 season (Fig. 2b). Under the RW rotation, both the RW-CB2 and RW-RB2 treatment increased the NAE of rice than other treatments in the Rice2019 season. Both the RW-RB2 and RW-RB2 treatments showed significantly higher NAE of wheat than RW-CU. Crop rotation had a significant effect on rice NAE in the Rice2020 season, while fertilization and the interaction between crop rotation and fertilization had no significant effects (Table S1).

3.2.Dynamics of soil inorganic nitrogen and plant nitrogen

Soil inorganic N increased to the highest at the middle of the tillering stage, then decreased to stability in the Rice2019 season (Fig. 3a). At the middle of the tillering stage, RG-CU, RR-CU, and RW-CU had higher soil inorganic N contents than other treatments, respectively (Table S2). The rice plant under the treatments of BBU also had higher plant N contents at tillering and elongation stages in the Rice2019 season (Fig. 3b, Table S4). In wheat season, soil inorganic N under RW-CU treatment increased to the highest at the middle of the tillering stage, while that under BBU treatments increased to the highest at flowering and mature stages (Fig. 3a). Reduction of N decreased the plant N contents of wheat at seeding stages (Fig. 3b). The dynamics of soil inorganic N were significantly changed after crop rotation (Fig. 3a). Soil inorganic N contents in all N treatments remained at a high level at seeding, tillering, elongation, and flowering stages. The plant N of rice in all N treatments were considerable at seeding, tillering, elongation, flowering, and mature stages (Fig. 3b). Soil inorganic N contents were significantly affected by crop rotation at elongation and flowering stages and significantly affected by fertilization at seeding, tillering, and mature stages in the Rice2020 season (Table S3). Crop rotation, fertilization, and interaction between them both had significant effects on rice plant N content at tillering and elongation stages in the Rice2020 season (Table S5).

3.3. Changes in soil properties

RG and RR rotations significantly increased soil pH under most fertilization treatments, while RW rotation had no significant influences on soil pH (Fig. S1a). In general, RG rotation increased soil pH more than RR rotation (Fig. 4a). Crop rotation, fertilization, and their interaction had significant effects on the changes in soil pH (Table S6). Three rotation treatments significantly increased SOC and TN under most fertilization treatments (Fig. S1b, c). The application of BBU could facilitate the increase of SOC under RG and RW rotations (Fig. 4b) and TN under RG and RR rotations (Fig. 4c) compared with CU. Both crop rotation, fertilization, and their interaction had no significant effects on the changes in SOC and TN (Table S6). RG-CB1, RR-CU, RW-WN, RW-CU, and RW-CB1 significantly altered the soil POXC contents (Fig. S1d). The N treatments weakened the increase of POXC in comparison to WN under RG rotation, while it facilitated the increase of POXC under RR and RW rotations (Fig. 4d). Only the interaction between crop rotation and fertilization showed a significant effect on the change in POXC (Table S6). Soil AK and available Al, Fe, Cu, Zn were increased, while soil available Ca, Mg, and Mn were decreased after crop rotation and fertilization (Fig. S2). Soil AP had no significant change in most of the treatments (Fig. S2). Crop rotation had significant effects on the changes in soil AK and available Ca, Mg, Al, Mn, Zn. Fertilization had significant effects on the changes in soil AP and available Ca, Mg, Al, Mn, Fe, Cu. Interaction between crop rotation and fertilization had significant effects on the changes in soil AP, AK, and available Mg, Al, Mn, Fe, Cu (Table S6).

3.4. Soil FTIR spectra

The FTIR-PAS spectra featured a broad peak at 3900-3700 cm^{-1} attributed to the stretching vibration (ν) of O-H from clay minerals (Table 1, Fig. 5a). A sharp peak of νO-H from clay minerals at 3620 cm^{-1} in FTIR-ATR spectra was also observed (Fig. 5b). The broadband ranged from 3600 to 3400 cm^{-1} attributed to νO-H from water, alcohols, phenols, carboxyl, and hydroxyl groups and νN-H from amides was both found in FTIR-PAS and FTIR-ATR spectra. The broadband at 3000-2800 cm^{-1} in FTIR-PAS spectra was dominated by νN-H from aliphatic methyl and methylene groups. The overtone of νCOH ranged from 2200 to 2000 cm^{-1} was derived from carbohydrates. The broadband ranged from 1720-1600 cm^{-1} was associated with νC-O from carboxylic acids and amides and νC-C from aromatics. The band at 1570-1540 cm^{-1} in FTIR-ATR spectra was dominated by νN-H and νC-N in plane from amide II. An obvious sharp peak at 1515 cm^{-1} in FTIR-PAS spectra attributed to νC-C from aromatics. The absorption band of νCO_3^{2-} from carbonates also was confirmed at 1500-1300 cm^{-1} in FTIR-ATR spectra. The shoulder at 1445-1350 cm^{-1} in FTIR-PAS spectra was assigned to νC-H from methyls. The νC-O and bending vibration (δ) of C-O in FTIR-ATR were derived from polysaccharides, nucleic acids, proteins, and carbohydrates. The FTIR-ATR showed an intensive peak at 990 cm^{-1} which was associated with νSi-O from clay minerals. A shoulder at 915 cm^{-1} attributed to δAl-OH from kaolinite and smectite.

The scatterplots of the first two PCA scores (PC1 and PC2) from FTIR-PAS and FTIR-ATR spectra indicated an obvious separation between soil samples before and after treatments (Fig. S5a, b). The PC1 and PC2 scores of soil FTIR-PAS spectra were mostly positive after treatments and both the PC1 and PC2 had positive loadings at the wavenumbers of νO-H, νO-H/νN-H, νC-C/νC-O, νC-C, νC-H, and νSi-O, (Fig. S5c), indicating that these functional groups in soil increased after crop rotation and fertilization. Soils after treatments mostly had negative PC2 scores for FTIR-ATR spectra and had positive PC2 loading at the wavenumbers of $\nu CO_3^{2-}$and νAl-OH (Fig. S5d), which suggested that soil CO_3^{2-} and Al-OH decreased after crop rotation and fertilization. We further applied PCA on the differential spectra of FTIR-PAS and FTIR-ATR. Crop rotation, fertilization, and their interaction had significant effects on PCA scores for FTIR-PAS differential spectra, while only their interaction had a significant effect on PCA scores of FTIR-ATR differential spectra (Fig. 5c, d). An obvious separation between soils after RG and RW rotations was observed according to PC1 for FTIR-PAS differential spectra. PC1 showed high positive scores for soils after RG rotation but high negative scores for soils after RW rotation (Fig. 6a). In addition, PC1 had high positive loadings at the wavenumbers of νC-C/νC-O and νC-C, and high negative loadings at the wavenumbers of νO-H/νN-H (Fig. S5). This suggested that RG rotation increased the soil functional group of O-H and N-H and decreased the soil functional groups of C-C, C-O, and C-C (Fig. 6).

SOC, TN, and POXC contents had a commonly significant relationship with the stretching vibrations of O-H (3900-3700 cm^{-1}) in the PLSR model of FTIR-PAS. However, SOC content showed a unique relationship with the stretching vibrations of C-C (1515 cm^{-1}) and POXC content presented a unique relationship with the stretching vibrations of C-H (1445-1350 cm^{-1}) in the PLSR model of FTIR-PAS (Fig. 5a). For FTIR-ATR, SOC, TN, and POXC contents were all significantly related to the stretching vibrations of CO_3^{2-} (1500-1300 cm^{-1}), C-O (1160 cm^{-1}), Si-O (1030-950 cm^{-1}), and the bending vibrations of Al-OH (915 cm^{-1}) in the PLSR model (Fig. 5b).

3.5. Structural equation model

SEM analysis indicated that three crop rotation patterns showed the different direct and indirect effects of fertilization on grain yield and NAE (Fig. 7). Under RG rotation, fertilization had a directly positive effect on NAE (0.453) but no significant effect on grain yield. The change of pH showed a negative effect on NAE (-0.337). The change of POXC presented negative effects on grain yield (-0.723) and NAE (-0.776), respectively. Under RR rotation, fertilization showed a directly negative effect on grain yield (-0.343) but no significant effect on NAE. Both the changes of pH and SOC had positive effects on grain yield and NAE under RR rotation. The change of POXC under RR rotation presented lower negative effects on grain yield (-0.502) and NAE (-0.427), respectively compared with that under RG rotation. Fertilization had no significant effect on grain yield and NAE under RW rotation. Only the change of SOC had a positive effect on NAE under RW rotation. In general, fertilization had no direct significant effect on the changes in soil pH, SOC, POXC, and nutrients under the three crop rotation patterns.

4. Discussion

4.1. Effects of crop rotation and fertilization ondynamics of soil inorganic N and plant N uptake

In the two rice seasons, CU treatments had higher soil inorganic N content than BBU treatments under the three crop rotations at the middle of the tillering and flowering stages because of the second and third topdressings of N (Fig. 3). The plant N contents, in contrast, were not significantly higher under CU treatments than BBU treatments at the middle of the tillering stage. Hydrolysis of urea in the soil is a rapid reaction, resulting in a sharp increase in the content of inorganic N in the soil in a short period (Skiba & Wainwright, 1984). However, limited by the N uptake rate of crops, only a small part of this high-concentration N is assimilated, and the rest is discharged into the environment through runoff, ammonia volatilization, etc. As shown in Fig. 3a, the soil inorganic N contents in CU treatments were significantly lower than that in BBU treatment at the elongation stage in the Rice2019 season (Table S2). The CU treatments also resulted in more inorganic N in the soil at the later periods of rice growth, which might cause late ripening or lodging of rice. Advantageously, inorganic N in the soils under BBU treatments was released slowly according to the N uptake rate of rice, which maintained inorganic N in the soil at an appropriate concentration. Therefore, application of BBU could increase the N uptake of rice and reduce the loss of reactive N into the hydrosphere and atmosphere, thereby increasing the NAE. There was no significant difference in the soil inorganic N between the single-dose and twice-split applications of BBU (Table S2). However, twice-split application of BBU slightly increased plant N content at seeding, tillering, and elongation stages. This demonstrated that twice-split application of BBU also improved suitability between the N demand and supply in rice, thereby increasing the NAE. In this study, the release period of N was delayed for wheat season, increasing soil inorganic N content in soil at the mature stage under BBU treatment (Fig. 3a). Although there was no obvious difference in soil inorganic N and plant N contents between different crop rotation systems at various stages (Table S2), the dynamic pattern of soil inorganic N significantly changed after the rotation season, especially under the BBU treatments (Fig. 3a). Soil inorganic N in BBU treatments under RG and RW rotations was higher than in CU treatment at the seeding stage, because of the residual N from the wheat season and the biologically fixed N from the green manure season. In addition, soil inorganic N in RG and RW rotations still presented a high concentration at the elongation stage. RG and RW rotations enhanced the retention capacity of soil fertility to supply sufficient N for rice even at the elongation stage. In addition, the residual N in RW rotation and biologically fixed N in RG rotation were released and mineralized in the Rice2020 season, respectively.

4.2. Effects of crop rotation and fertilization on the changes in soil properties

Soil pH plays an important role in crop production, nutrient chemistry, soil organisms, and shaping plant community composition (Sun et al., 2020). Both CU and BBU fertilizations resulted in a significant short-term increase in soil pH under RG and RR rotations (Figs. 4a, S1a), which was caused by the production of OH^- from the hydrolysis of urea and the limitation of nitrification under paddy soil (Curtin, Peterson, Qiu, & Fraser, 2020). However, fertilization did not significantly increase the soil pH under RW rotation. This might be due to the strong nitrification process in the aerobic environment during the wheat cropping season in which more H^+ was generated to counteract the increase in pH from paddy rice season. SOC is critical for soil structure and workability, the ability of soils to store nutrients and water, and for the global C cycle (Sun et al., 2020). In this study, almost all treatments significantly enhanced the SOC, which was dominated by the retention of straw residues (Y. Zhao et al., 2018). The previous study indicated that SOC stock changes in Chinese croplands were positively correlated with N fertilizer input and crop residue C input (Y. Zhao et al., 2018). BBU enhanced the plant growth leading to more inputs of C from straw and roots, which presumably contributed to the higher SOC in BBU fertilizations (Pampolino, Laureles, Gines, & Buresh, 2008). Generally, crop rotation had a direct impact on the dynamic of SOC by altering the input C to the soil and the soil microbial activity (D'Acunto, Andrade, Poggio, & Semmartin, 2018; Osanai, Knox, Nachimuthu, & Wilson, 2021). However, our result showed that there was no significant difference in the changes in SOC among the three cropping rotations, which might be due to the short experiment period. Similarly, soil TN contents were increased after crop rotation and fertilization, which presumably was attributed to the straw turnover. The changes in soil TN contents under RG and RR rotations were higher than that under RW rotation. This difference was caused by the additional N fixed by Chinese milk vetch during RG rotation and a greater amount of residual including rape straw and grain during RR rotation (Alam, Bell, Haque, Islam, & Kader, 2020). Soil POXC, which stands for labile SOC fraction, is useful as an indicator for assessing soil health and C sequestration potential (Lucas & Weil, 2021). Both CU and BBU fertilizations significantly increased the soil POXC contents compared with WN treatment except for RG rotation. The change in soil POXC content was positively correlated with the changes in SOC and TN contents (Fig. S3). Fertilization enhanced the soil C input by improving crop growth and promoted the decomposition of stubble and straw residuals. The decreases of soil AP and available Mg were mainly caused by crop uptake and the increase of available Zn mostly due to the application of Zn fertilizer. Other available trace elements such as Mn, Fe, and Cu had a positive correlation with SOC and TN, indicating that the availability of these elements was related to SOC and TN contents.

4.3. Effects of crop rotation and fertilization on the organic and mineral functional groups

The soil FTIR-PAS and FTIR-ATR spectra could discover the changes in the molecular structure of soil organic and mineral as the adsorption bands of FTIR had a high correlation with SOC (R^2=0.617, 0.650), TN (R^2=0.585, 0.606), and POXC (R^2=0.606, 0.584) in the PLSR model (Fig. 6b). According to the variable in projections of POXC in the PLSR model, the POXC content showed a unique correlation with the bands of νC-H from aliphatic and methyl compounds which were considered as intrinsically easily degradable (Smidt & Meissl, 2007). Peltre, Bruun, Du, Thomsen, and Jensen (2014) also reported a chiefly positive correlation between the labile fraction of SOC and the similar band at 1520-1400 cm^{-1}. Moreover, the POXC content was also correlated with the bands of νC-O (1160 cm^{-1}) and δC-O (1050 cm^{-1}) which attributed to polysaccharides, nucleic acids, proteins, and carbohydrates. The polysaccharides and carbohydrates are considered intrinsically labile (Amelung, Brodowski, Sandhage-Hofmann, & Bol, 2008). The soil νC-H band in some treatments significantly increased under RG and RR rotations while it had no significant change under RW rotation (Fig. 6), which was consistent with the change in soil POXC content. These results suggested that fertilization under RG and RR rotations increased the labile fraction of SOC. The bands of νO-H/νN-H at 3600-3400 cm^{-1}attributed to water, alcohols, phenols, carboxyl, hydroxyl groups, and amides also significantly increased under the RG rotation. An increase of amides groups under RG rotation confirmed a greater increase of TN under RG rotation which potentially attributed to the biological N fixation of rhizobia on Chinese milk vetch. The νC-C/νC-O and νC-C bands at 1720-1600 cm^{-1} and 1515 cm^{-1} were associated with carboxylic acids, amides, and aromatics, respectively. These compounds are considered to be degradation-resistant due to the recalcitrant nature of aromatic structures and due to the organo-mineral associations (Lützow et al., 2006). The organo-mineral associations are possibly formed through polyvalent cation bridges with clay surfaces and enhancing hydrophobicity to resist the microorganisms and their enzymes (Peltre et al., 2014). In this study, the intensities of νC-C and νC-O bands were significantly reduced after RG rotation rather than RR and RW rotations, suggesting RG rotation reduced the relative abundance of the stabilized SOC. In addition, the decrease of νCO_3^{2-} and δAl-OH demonstrated that the relative abundances of soil carbonates, kaolinite, and smectite decreased after crop rotation and fertilization, especially for the fertilization treatments. The decrease of these soil minerals possibly was caused by the dilution effect by increased organic matter in the soil.

4.4. Effects of crop rotation and fertilization on rice grain yield and NAE

In this study, crop rotation and fertilization affected grain yield and NAE directly by regulating N supply in the soil on the one hand and indirectly by altering soil chemical property on the other. In general, fertilization showed more direct effects through regulating N supply while crop rotation had more indirect effects by altering soil chemical property. By regulating the release of N, BBU maintained the soil inorganic N at a high and stable level during the period of rice growth, especially during the elongation stage, which not only improved the N uptake of the rice plant but also effectively reduced the losses of reactive N into the environment. As a result, the grain yield and NAE were improved. Twice-split application of BBU improved grain yield and NAE because it was better to balance the N requirement of rice and supply, especially in the soil with poor fertility retention. However, reduction of N fertilization rate was adverse to rice growth and resulted in unsatisfactory grain yield because of the relatively low basic soil fertility. Crop rotation had no direct effect on grain yield and NAE but showed significant indirect impacts on the changes in soil properties. Under RG rotation, changes in soil pH and POXC had significant negative effects on grain yield and NAE (Fig. 7a). As mentioned above, RG rotation increased soil pH and the labile fraction of SOC most and decreased the stable SOC. In other words, the strong increase in pH and degradation of stable SOC were adverse to improving grain yield and NAE under RG rotation. RR rotation indirectly affected grain yield and NAE by changing soil properties as strong correlations between grain yield and NAE and changes in soil pH, SOC, and POXC were observed. Only the change in SOC showed a significant effect on NAE under RW rotation, indicating the weakly indirect impact of RW rotation on grain yield and NAE. On the whole, application of BBU had direct positive effects on improving grain yield and NAE under RG and RW rotations but direct negative effects under RR rotation.

5. Conclusions

The BBU could controlla bly release N to improve the N uptake according to the requirement of rice during various growth stages. Accordingly, fertilization of BBU with twice-split application increased both the rice grain yield and NAE in comparison to conventional urea. At the same time, crop rotation combined with fertilization significantly increased the soil pH, SOC, TN, and POXC, resulting in the enhancement of soil fertility retention. The RG rotation showed a higher increase in soil pH and TN than other crop rotations, which benefited from the biological nitrogen fixation of Chinese milk vetch. FTIR spectra indicated that RG rotation combined with fertilization significantly increased the aliphatic and methyl compounds which were considered as the labile fraction of SOC and reduced the relative abundance of carboxylic acids, amides, and aromatics which were regarded as the stabled fraction of SOC. Crop rotation also significantly reduced the soil carbonate. The rice grain yield and NAE were influenced more by the changes in soil properties under RG and RR rotations than that under RW rotation.

Declaration of competing interest

The authors declare that they have no known competing financial interests or personal relationships that could have appeared to influence the work reported in this paper.

Acknowledgments

This work was supported by the Strategic Priority Research Program of the Chinese Academy of Sciences (XDA28040500, XDA28120400) and the "STS" Project from Chinese Academy of Sciences (KFJSTS-QYZX-047).

References

Alam, M. K., Bell, R. W., Haque, M. E., Islam, M. A., & Kader, M. A. (2020). Soil nitrogen storage and availability to crops are increased by conservation agriculture practices in rice-based cropping systems in the Eastern Gangetic Plains. *Field Crops Research, 250* , 107764.*https://doi.org/10.1016/j.fcr.2020.107764*

Amelung, W., Brodowski, S., Sandhage-Hofmann, A., & Bol, R. (2008). Chapter 6 Combining biomarker with dtable isotope analyses for assessing the transformation and turnover of soil organic matter. In*Advances in Agronomy* (Vol. 100, pp. 155-250): Academic Press.

Bender, S. F., Wagg, C., & van der Heijden, M. G. A. (2016). An underground revolution: Biodiversity and soil ecological engineering for agricultural sustainability. *Trends in Ecology & Evolution, 31* (6), 440-452.*https://doi.org/10.1016/j.tree.2016.02.016*

Blair, G., Lefroy, R., & Lisle, L. (1995). Soil carbon fractions based on their degree of oxidation, and the development of a carbon management index for agricultural systems. *Australian Journal of Agricultural Research, 46* (7), 1459-1466.*https://doi.org/10.1071/AR9951459*

Calderón, F., Haddix, M., Conant, R., Magrini-Bair, K., & Paul, E. (2013). Diffuse-reflectance fourier-transform mid-infrared spectroscopy as a method of characterizing changes in soil organic matter. *Soil Science Society of America Journal, 77* (5), 1591-1600.*https://doi.org/10.2136/sssaj2013.04.0131*

Chen, J., Lü, S., Zhang, Z., Zhao, X., Li, X., Ning, P., & Liu, M. (2018). Environmentally friendly fertilizers: A review of materials used and their effects on the environment. *Science of the Total Environment, 613-614* , 829-839.*https://doi.org/10.1016/j.scitotenv.2017.09.186*

Chen, L., Liu, M., Ali, A., Zhou, Q., Zhan, S., Chen, Y., . . . Zeng, Y. (2020). Effects of biochar on paddy soil fertility under different water management modes. *Journal of Soil Science and Plant Nutrition, 20* (4), 1810-1818.*https://doi.org/10.1007/s42729-020-00252-8*

Churchman, G. J., Foster, R. C., D'Acqui, L. P., Janik, L. J., Skjemstad, J. O., Merry, R. H., & Weissmann, D. A. (2010). Effect of land-use history on the potential for carbon sequestration in an Alfisol. *Soil and Tillage Research, 109* (1), 23-35.*https://doi.org/10.1016/j.still.2010.03.012*

Curtin, D., Peterson, M. E., Qiu, W., & Fraser, P. M. (2020). Predicting soil pH changes in response to application of urea and sheep urine. *Journal of Environmental Quality, 49* (5), 1445-1452.*https://doi.org/10.1002/jeq2.20130*

D'Acunto, L., Andrade, J. F., Poggio, S. L., & Semmartin, M. (2018). Diversifying crop rotation increased metabolic soil diversity and activity of the microbial community. *Agriculture, Ecosystems & Environment, 257* , 159-164.*https://doi.org/10.1016/j.agee.2018.02.011*

Du, C., Goyne, K. W., Miles, R. J., & Zhou, J. (2014). A 1915–2011 microscale record of soil organic matter under wheat cultivation using FTIR-PAS depth-profiling. *Agronomy for Sustainable Development, 34* (4), 803-811.*https://doi.org/10.1007/s13593-013-0201-6*

Du, C., Linker, R., & Shaviv, A. (2007). Characterization of soils using photoacoustic mid-infrared spectroscopy. *Applied Spectroscopy, 61* (10), 1063-1067.*https://doi.org/10.1366/000370207782217743*

Ellerbrock, R. H., & Gerke, H. H. (2004). Characterizing organic matter of soil aggregate coatings and biopores by Fourier transform infrared spectroscopy. *European Journal of Soil Science, 55* (2), 219-228.*https://doi.org/10.1046/j.1365-2389.2004.00593.x*

Fu, H., Duan, Y., Zhu, P., Gao, H., & Xu, M. (2021).^{15}N fate in maize cropping system in response to black soil fertility improvement in China. *Agronomy Journal, 113* (5), 4323-4333.*https://doi.org/10.1002/agj2.20794*

Gao, Y., Song, X., Liu, K., Li, T., Zheng, W., Wang, Y., . . . Miao, T. (2021). Mixture of controlled-release and conventional urea fertilizer application changed soil aggregate stability, humic acid molecular composition, and maize nitrogen uptake. *Science of the Total Environment, 789* , 147778.*https://doi.org/10.1016/j.scitotenv.2021.147778*

German, R. N., Thompson, C. E., & Benton, T. G. (2017). Relationships among multiple aspects of agriculture's environmental impact and productivity: a meta-analysis to guide sustainable agriculture.*Biological Reviews, 92* (2), 716-738.*https://doi.org/10.1111/brv.12251*

Ghosh, P. K., Hazra, K. K., Venkatesh, M. S., Praharaj, C. S., Kumar, N., Nath, C. P., . . . Singh, S. S. (2020). Grain legume inclusion in cereal-cereal rotation increased base crop productivity in the long run.*Experimental Agriculture, 56* (1), 142-158.*https://doi.org/10.1017/S0014479719000243*

Giacometti, C., Mazzon, M., Cavani, L., Triberti, L., Baldoni, G., Ciavatta, C., & Marzadori, C. (2021). Rotation and fertilization effects on soil quality and yields in a long term field experiment.*Agronomy, 11* (4), 636.*https://doi.org/10.3390/agronomy11040636*

Gong, Z., Lei, W. J., Chen, Z. C., Gao, Y. X., Zeng, S. G., Zhang, G. L., . . . Li, S. G. (2001). *Chinese soil taxonomy* . Beijing: Science Press.

Guo, C., Ren, T., Li, P., Wang, B., Zou, J., Hussain, S., . . . Li, X. (2019). Producing more grain yield of rice with less ammonia volatilization and greenhouse gases emission using slow/controlled-release urea. *Environmental Science and Pollution Research, 26* (3), 2569-2579.*https://doi.org/10.1007/s11356-018-3792-2*

Hu, H., Ning, T., Li, Z., Han, H., Zhang, Z., Qin, S., & Zheng, Y. (2013). Coupling effects of urea types and subsoiling on nitrogen-water use and yield of different varieties of maize in northern China.*Field Crops Research, 142* , 85-94.*https://doi.org/10.1016/j.fcr.2012.12.001*

Huang, X., Li, S., Li, S., Ye, G., Lu, L., Zhang, L., . . . Liu, J. (2019). The effects of biochar and dredged sediments on soil structure and fertility promote the growth, photosynthetic and rhizosphere microbial diversity of *Phragmites communis (Cav.) Trin. ex Steud .Science of the Total Environment, 697* , 134073.*https://doi.org/10.1016/j.scitotenv.2019.134073*

Jackson, M. L. (1958). *Soil chemical analysis* (Vol. 85). New Delhi, India: Prentice Hall, Inc., Englewood Cliffs, NJ.

Janik, L. J., Skjemstad, J. O., Shepherd, K. D., & Spouncer, L. R. (2007). The prediction of soil carbon fractions using mid-infrared-partial least square analysis. *Soil Research, 45* (2), 73-81.*https://doi.org/10.1071/SR06083*

Leifeld, J. (2006). Application of diffuse reflectance FT-IR spectroscopy and partial least-squares regression to predict NMR properties of soil organic matter. *European Journal of Soil Science, 57* (6), 846-857.*https://doi.org/10.1111/j.1365-2389.2005.00776.x*

Li, J., Liu, Y., & Yang, Y. (2018). Land use change and effect analysis of tideland reclamation in Hangzhou Bay. *Journal of Mountain Science, 15* (2), 394-405.*https://doi.org/10.1007/s11629-017-4542-5*

Liu, D., Song, C., Fang, C., Xin, Z., Xi, J., & Lu, Y. (2021). A recommended nitrogen application strategy for high crop yield and low environmental pollution at a basin scale. *Science of the Total Environment, 792* , 148464.*https://doi.org/10.1016/j.scitotenv.2021.148464*

Lucas, S., & Weil, R. (2021). Can permanganate oxidizable carbon predict soil function responses to soil organic matter management?*Soil Science Society of America Journal, 85* (5), 1768-1784.*https://doi.org/10.1002/saj2.20282*

Lützow, M. v., Kögel-Knabner, I., Ekschmitt, K., Matzner, E., Guggenberger, G., Marschner, B., & Flessa, H. (2006). Stabilization of organic matter in temperate soils: mechanisms and their relevance under different soil conditions-a review. *European Journal of Soil Science, 57* (4), 426-445.*https://doi.org/10.1111/j.1365-2389.2006.00809.x*

Madejová, J. (2003). FTIR techniques in clay mineral studies.*Vibrational Spectroscopy, 31* (1), 1-10.*https://doi.org/10.1016/S0924-2031(02)00065-6*

Malobane, M. E., Nciizah, A. D., Mudau, F. N., & Wakindiki, I. I. C. (2020). Tillage, crop rotation and crop residue management effects on nutrient availability in a sweet sorghum-based cropping system in marginal soils of South Africa. *Agronomy, 10* (6), 776.*https://doi.org/10.3390/agronomy10060776*

Movasaghi, Z., Rehman, S., & ur Rehman, D. I. (2008). Fourier transform infrared (FTIR) dpectroscopy of biological tissues. *Applied Spectroscopy Reviews, 43* (2), 134-179.*https://doi.org/10.1080/05704920701829043*

Nayak, P. S., & Singh, B. K. (2007). Instrumental characterization of clay by XRF, XRD and FTIR. *Bulletin of Materials Science, 30* (3), 235-238.*https://doi.org/10.1007/s12034-007-0042-5*

Olsen, S. R. (1954). *Estimation of available phosphorus in soils by extraction with sodium bicarbonate.* Paper presented at the USDA Circular, Washington, DC, USA.

Osanai, Y., Knox, O., Nachimuthu, G., & Wilson, B. (2021). Contrasting agricultural management effects on soil organic carbon dynamics between topsoil and subsoil. *Soil Research, 59* (1), 24-33.*https://doi.org/10.1071/SR19379*

Pampolino, M. F., Laureles, E. V., Gines, H. C., & Buresh, R. J. (2008). Soil carbon and nitrogen changes in long-term continuous lowland rice cropping. *Soil Science Society of America Journal, 72* (3), 798-807.*https://doi.org/10.2136/sssaj2006.0334*

Pansu, M., & Gautheyrou, J. (2006). Organic and total C, N (H, O, S) analysis. In *Handbook of soil analysis: Mineralogical, organic and inorganic methods* (pp. 327-370). Berlin, Heidelberg: Springer Berlin Heidelberg.

Pedersen, J. A., Simpson, M. A., Bockheim, J. G., & Kumar, K. (2011). Characterization of soil organic carbon in drained thaw-lake basins of Arctic Alaska using NMR and FTIR photoacoustic spectroscopy.*Organic Geochemistry, 42* (8), 947-954.*https://doi.org/10.1016/j.orggeochem.2011.04.003*

Peltre, C., Bruun, S., Du, C., Thomsen, I. K., & Jensen, L. S. (2014). Assessing soil constituents and labile soil organic carbon by mid-infrared photoacoustic spectroscopy. *Soil Biology and Biochemistry, 77* , 41-50.*https://doi.org/10.1016/j.soilbio.2014.06.022*

Piao, S., Ciais, P., Huang, Y., Shen, Z., Peng, S., Li, J., . . . Fang, J. (2010). The impacts of climate change on water resources and agriculture in China. *Nature, 467* (7311), 43-51.*https://doi.org/10.1038/nature09364*

R Development Core Team. (2018). R: a language and environment for statistical computing. *R Foundation for Statistical Computing.*Retrieved from*https://www.R-project.org/.*

Rossel, R. A. V., & Behrens, T. (2010). Using data mining to model and interpret soil diffuse reflectance spectra. *Geoderma, 158* (1), 46-54.*https://doi.org/10.1016/j.geoderma.2009.12.025*

Shen, Y., Du, C., Zhou, J., & Ma, F. (2017). Application of nano Fe(III)-tannic scid complexes in modifying aqueous acrylic latex for controlled-release coated urea. *Journal of Agricultural and Food Chemistry, 65* (5), 1030-1036.*https://doi.org/10.1021/acs.jafc.6b05274*

Sindelar, A. J., Schmer, M. R., Jin, V. L., Wienhold, B. J., & Varvel, G. E. (2016). Crop rotation affects corn, grain sorghum, and soybean yields and nitrogen recovery. *Agronomy Journal, 108* (4), 1592-1602.*https://doi.org/10.2134/agronj2016.01.0005*

Skiba, U., & Wainwright, M. (1984). Urea hydrolysis and transformations in coastal dune sands and soil. *Plant and Soil, 82* (1), 117-123.*https://doi.org/10.1007/BF02220775*

Smidt, E., & Meissl, K. (2007). The applicability of Fourier transform infrared (FT-IR) spectroscopy in waste management. *Waste Management, 27* (2), 268-276.*https://doi.org/10.1016/j.wasman.2006.01.016*

Soriano-Disla, J. M., Janik, L. J., Viscarra Rossel, R. A., Macdonald, L. M., & McLaughlin, M. J. (2014). The performance of visible, near-, and mid-infrared reflectance spectroscopy for prediction of soil physical, chemical, and biological properties. *Applied Spectroscopy Reviews, 49* (2), 139-186.*https://doi.org/10.1080/05704928.2013.811081*

Stewart, Z. P., Pierzynski, G. M., Middendorf, B. J., & Prasad, P. V. V. (2020). Approaches to improve soil fertility in sub-Saharan Africa.*Journal of Experimental Botany, 71* (2), 632-641.*https://doi.org/10.1093/jxb/erz446*

Sun, Y., Guo, G., Shi, H., Liu, M., Keith, A., Li, H., & Jones, K. C. (2020). Decadal shifts in soil pH and organic matter differ between land uses in contrasting regions in China. *Science of the Total Environment, 740* , 139904.*https://doi.org/10.1016/j.scitotenv.2020.139904*

Thomas, G. W. (1996). Soil pH and soil acidity. In *Methods of Soil Analysis* (pp. 475-490).

Tomaszewska, M., & Jarosiewicz, A. (2002). Use of polysulfone in controlled-release NPK fertilizer formulations. *Journal of Agricultural and Food Chemistry, 50* , 4634-4639.*https://doi.org/10.1021/jf0116808*

Viscarra Rossel, R. A., & Behrens, T. (2010). Using data mining to model and interpret soil diffuse reflectance spectra. *Geoderma, 158* (1), 46-54.*https://doi.org/10.1016/j.geoderma.2009.12.025*

Walkley, A., & Black, I. A. (1934). An examination of Degtjare method for determining soil organic matter, and a proposed modification of the chromic acid titration method. *Soil Science, 37* (1), 29-38.*https://doi.org/10.1097/00010694-193401000-00003*

Xing, Z., Tian, K., Du, C., Li, C., Zhou, J., & Chen, Z. (2019). Agricultural soil characterization by FTIR spectroscopy at micrometer scales: Depth profiling by photoacoustic spectroscopy. *Geoderma, 335* , 94-103.*https://doi.org/10.1016/j.geoderma.2018.08.003*

Xu, X., Du, C., Ma, F., Shen, Y., & Zhou, J. (2020). Forensic soil analysis using laser-induced breakdown spectroscopy (LIBS) and Fourier transform infrared total attenuated reflectance spectroscopy (FTIR-ATR): Principles and case studies. *Forensic Science International, 310* , 110222.*https://doi.org/10.1016/j.forsciint.2020.110222*

Yang, J., & Lin, Y. (2019). Spatiotemporal evolution and driving factors of fertilizer reduction control in Zhejiang Province.*Science of the Total Environment, 660* , 650-659.*https://doi.org/10.1016/j.scitotenv.2018.12.420*

Zeng, Z., Lu, Z. Y., Jiang, Y., Zhang, K., Yang, Y., & Zhao, P. Y. (2016). Legume-cereal crop rotation systems in China. In B. L. Ma (Ed.),*Crop rotations: farming practices, monitoring and environmental benefits* (pp. 51-70). New York: Nova Science Publishers, Inc.

Zhao, J., Yang, Y., Zhang, K., Jeong, J., Zeng, Z., & Zang, H. (2020). Does crop rotation yield more in China? A meta-analysis. *Field Crops Research, 245* , 107659.*https://doi.org/10.1016/j.fcr.2019.107659*

Zhao, Y., Wang, M., Hu, S., Zhang, X., Ouyang, Z., Zhang, G., . . . Shi, X. (2018). Economics- and policy-driven organic carbon input enhancement dominates soil organic carbon accumulation in Chinese croplands.*Proceedings of the National Academy of Sciences of the United States of America, 115* (16), 4045-4050.*https://doi.org/10.1073/pnas.1700292114*

Table 1

Assignment of the absorption bands in FTIR-PAS and FTIR-ATR spectra.

Wavenumber (cm^{-1})	Wavenumber (cm^{-1})	Vibration	Functional group or component
FTIR-PAS	FTIR-ATR		
3900-3700	-	νO-H	Clay minerals (Churchman et al., 2010; Xing et al., 201
	3620	νO-H	Clay minerals (Xu, Du, Ma, Shen, & Zhou, 2020)
3600-3400	3600-3000	νO-H, N-H	Water, alcohols, and phenols; carboxyl and hydroxyl gr
3000-2800	-	νC-H	Aliphatic methyl and methylene groups (Ellerbrock &
2200-2000	2200-2000	Overtone νCOH	Carbohydrates (Janik, Skjemstad, Shepherd, & Spounc
1720-1600	1720-1600	νC-O, νC-C	Carboxylic acids; amides; Aromatics (Changwen Du, G
-	1570–1540	νN-H, νC-N in plane	Amide II (Calderón, Haddix, Conant, Magrini-Bair, &
1515	1515	νC-C	Aromatics (Calderón et al., 2013)
-	1500-1300	νCO_3^{2-}	Carbonates (Viscarra Rossel & Behrens, 2010)
1445-1350	-	νC-H	Methyls (Janik et al., 2007; Rossel & Behrens, 2010)
-	1160	νC-O	Polysaccharides, nucleic acids, proteins (Calderón et al
-	1050	δC-O	Carbohydrates (Movasaghi, Rehman, & ur Rehman, 20
1030-950	990	νSi-O	Clay minerals (Madejová, 2003)
-	915	δAl-OH	Kaolinite and smectite (Viscarra Rossel & Behrens, 20
850	-	NH_2 out of plane	Primary amine (Smidt & Meissl, 2007)
-	770	NH_2 out of plane	Primary amine (Nayak & Singh, 2007)

Where ν and δ denote stretching vibration and bending vibration, respectively.

Figure legends

Fig. 1. Geographic coordinates and maps showing of the split-plot design in this experiment. WN, withdrawal of N fertilizer; CU, farmer's conventional urea fertilizing practice with the thrice-split application; CB1, single-dose application of bulk blending urea (BBU) with the conventional amount of N; CB2, twice-split application of BBU with the conventional amount of N; RB1, single-dose application of BBU with 20% reduction of N; and RB2, twice-split application of BBU with 20% reduction of N.

Fig. 2. Grain yields (a) and nitrogen agronomic efficiencies (NAE, b) of rice and wheat as affected by crop rotation and fertilization. Different lowercase letters present the statistical differences among different treatments at $P < 0.05$ according to the least significant difference (LSD) method.

Fig. 3. Dynamics of soil total inorganic N contents (a) and plant N contents (b) at various growth stages under different treatments. Rice2019, rice growth season in 2019; Wheat, wheat growth season from 2019 to 2020; Rice2020, rice growth season in 2020.

Fig. 4. Changes in soil pH (a), soil organic carbon (SOC, b), total N (TN, c), and permanganate oxidize carbon (POXC, d) after different treatments. Different lowercase letters present the statistical differences among different treatments at $P< 0.05$ according to the least significant difference (LSD) method.

Fig. 5. PLSR (a, b) and PCA (c, d) analyses of soil FTIR-PAS (a, c) and FTIR-ATR (b, d) spectra. The bar codes under the spectral curves show wavenumbers of the top 10% spectral variables according to the scores of variables important in projections in the PLSR model. The density curves along the axis show the independent distributions of the first and second components under different fertilizations. R^2 values represent the independent and interactional effects of crop rotation and fertilization according to the two-way permutational multivariate analysis of variance (PERMANOVA). Significance levels are denoted with * $P < 0.05$, **$P < 0.01$, and *** $P < 0.001$, respectively.

Fig. 6. Comparison of the intensities of soil FTIR-PAS bands as affected by different treatments. Significance levels are denoted with *$P < 0.05$, ** $P < 0.01$, and *** $P< 0.001$, respectively according to paired-samples T-test.

Fig. 7. Structural equation modeling shows the effects of fertilization, and soil properties on the grain yield and NAE under different crop rotation patterns. Green lines indicate positive effects, while red lines indicate negative effects. Gray lines indicate nonsignificant effects. The width of arrows indicates the strength of significant standardized path coefficients. Soil nutrients include soil total nitrogen (TN), NH_4^+-N, NO_3^--N, available phosphorus (AP), available potassium (AK), and available- Ca, Mg, Mn, Fe, Cu, Zn.

Supplementary materials

Table S1. Two-way ANOVA analysis of the crop rotation (R) and fertilization (F) on grain yield and NAE of paddy rice 2020 growing season.

Table S2. Dynamics of soil total inorganic nitrogen contents in different crop growing periods under various treatments.

Table S3. Two-way ANOVA analysis the crop rotation (R) and fertilization (F) on soil total inorganic nitrogen contents in 2019 and 2020 growing seasons.

Table S4. Dynamics of plant nitrogen contents in different crop growing periods under various treatments.

Table S5. Two-way ANOVA analysis of the crop rotation (R) and fertilization (F) on plant nitrogen contents in 2019 and 2020 growing seasons.

Table S6. Two-way ANOVA analysis the crop rotation (R) and fertilization (F) on the change of soil properties after 2019 and 2020 growing seasons.

Fig. S1. Comparison of soil pH (a), soil organic carbon (SOC, b), total nitrogen (TN, c), and permanganate oxidizes carbon (POXC, d) between before and after treatments. Significance levels are denoted with * $P < 0.05$, ** $P < 0.01$, and ***$P < 0.001$, respectively according to paired-samples T-test.

Fig. S2. Comparison of soil available medium and trace elements between before and after treatments. Significance levels are denoted with * $P < 0.05$, ** $P < 0.01$, and ***$P < 0.001$, respectively according to paired-samples T-test.

Fig. S3. Pearson correlations between various soil properties. Significance levels are denoted with * $P < 0.05$, **$P < 0.01$, and *** $P < 0.001$, respectively.

Fig. S4. The first (PC1) and second (PC2) loadings in PCA of differential spectra as changed by wavenumber.

Fig. S5. Comparison of the intensities of soil FTIR-PAS bands as affected by different treatments. Significance levels are denoted with * $P < 0.05$, ** $P < 0.01$, and ***$P < 0.001$, respectively according to paired-samples T-test.

Fig. S6. Comparison of the intensities of soil FTIR-ATR bands as affected by different treatments. Significance levels are denoted with * $P < 0.05$, ** $P < 0.01$, and ***$P < 0.001$, respectively according to paired-samples T-test.

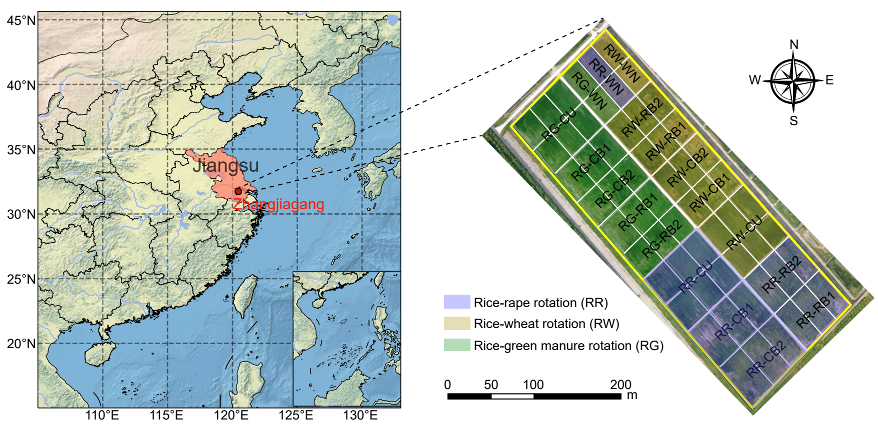

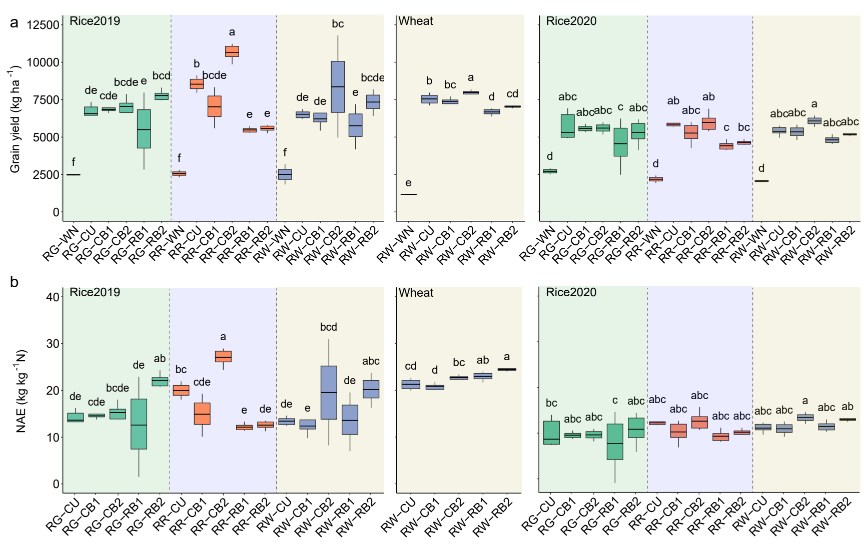

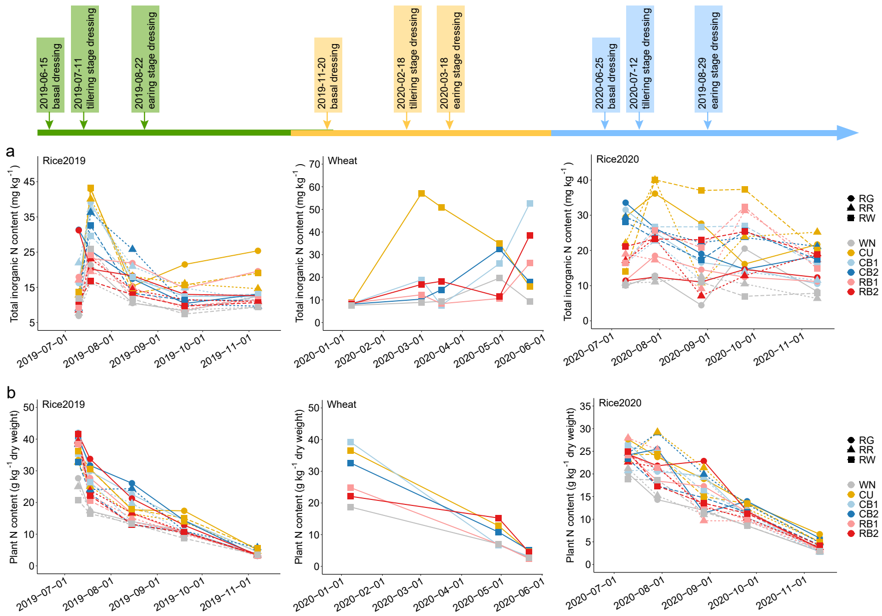
2019-06-15 basal dressing
2019-07-11 tillering stage dressing
2019-08-22 earing stage dressing
2019-11-20 basal dressing
2020-02-18 tillering stage dressing
2020-03-18 earing stage dressing
2020-06-25 basal dressing
2020-07-12 tillering stage dressing
2019-08-29 earing stage dressing
a
Rice2019
Wheat
Rice2020
Total inorganic N content (mg kg^{-1})
b
Plant N content (g kg^{-1} dry weight)
RG
RR
RW
WN
CU
CB1
CB2
RB1
RB2

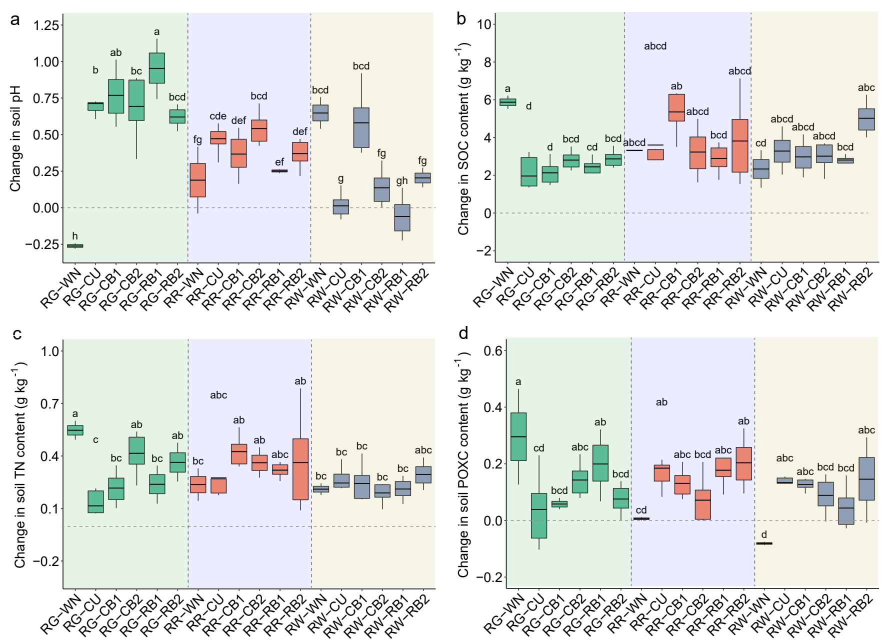
a
Change in soil pH
b
Change in SOC content (g kg^{-1})
c
Change in soil TN content (g kg^{-1})
d
Change in soil POXC content (g kg^{-1})
RG-WN
RG-CU
RG-CB1
RG-CB2
RG-RB1
RG-RB2
RR-WN
RR-CU
RR-CB1
RR-CB2
RR-RB1
RR-RB2
RW-WN
RW-CU
RW-CB1
RW-CB2
RW-RB1
RW-RB2

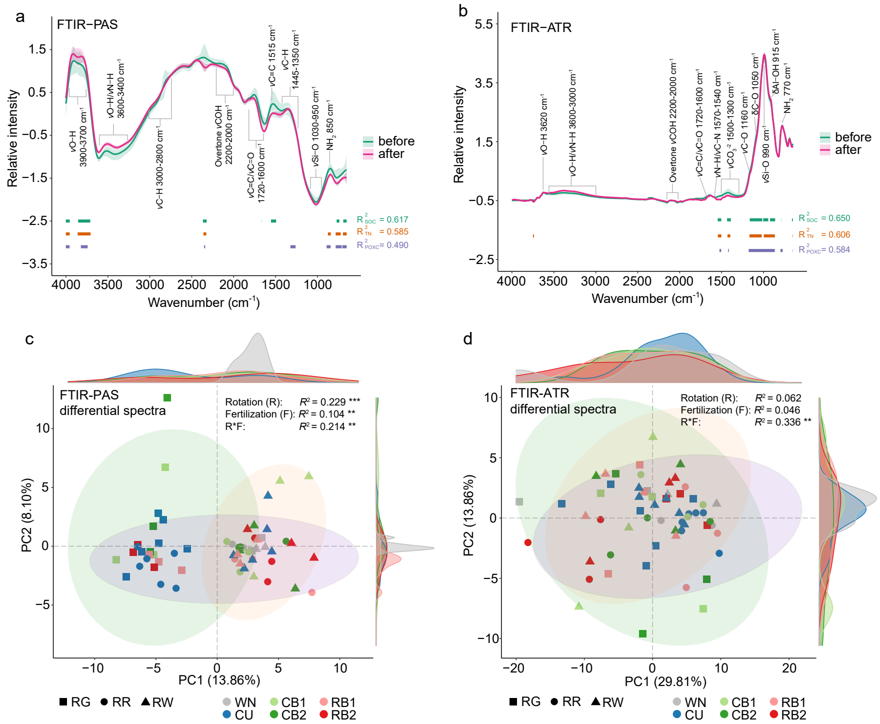
a
FTIR−PAS
Relative intensity
Wavenumber (cm-1)
before
after
b
FTIR−ATR
c
FTIR−PAS
differential spectra
Rotation (R): R² = 0.229 ***
Fertilization (F): R² = 0.104 **
R*F: R² = 0.214 **
PC1 (13.86%)
PC2 (8.10%)
d
FTIR−ATR
differential spectra
Rotation (R): R² = 0.062
Fertilization (F): R² = 0.046
R*F: R² = 0.336 **
PC1 (29.81%)
PC2 (13.86%)
RG RR RW
WN CU CB1 CB2 RB1 RB2

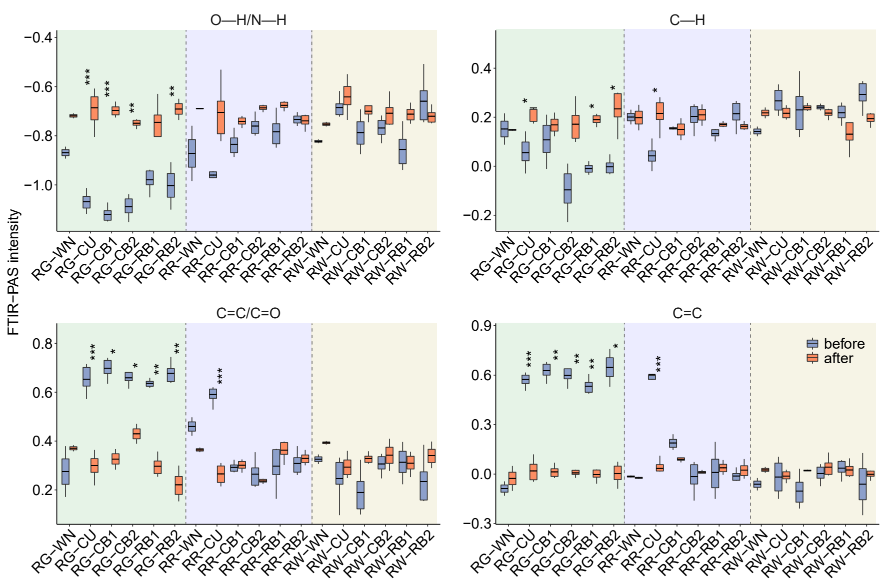
O—H/N—H
C—H
C=C/C=O
C=C
FTIR−PAS intensity
before
after

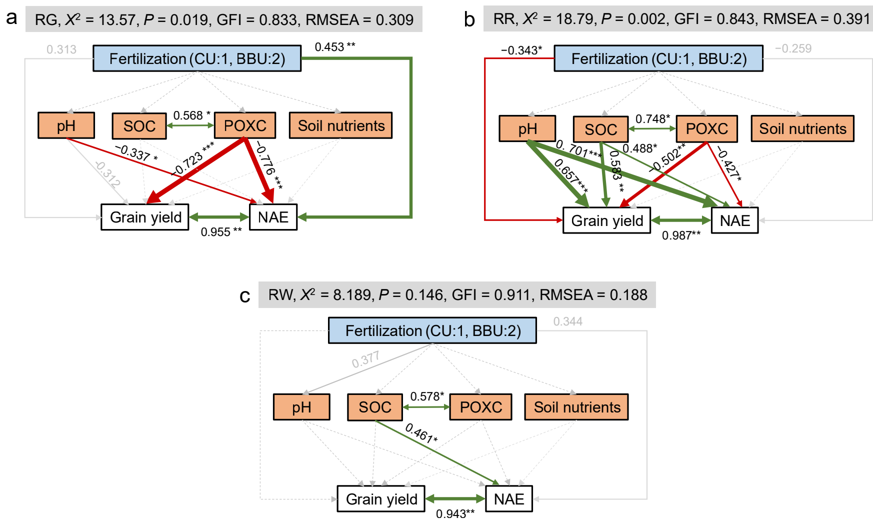
a
RG, X^2 = 13.57, P = 0.019, GFI = 0.833, RMSEA = 0.309
0.313
Fertilization (CU:1, BBU:2)
0.453 **
pH
SOC
0.568 *
POXC
Soil nutrients
−0.337 *
−0.723 ***
−0.776 ***
−0.312
Grain yield
NAE
0.955 **
b
RR, X^2 = 18.79, P = 0.002, GFI = 0.843, RMSEA = 0.391
−0.343*
Fertilization (CU:1, BBU:2)
−0.259
pH
SOC
0.748*
POXC
Soil nutrients
0.701***
0.657***
0.583 **
0.488*
−0.502**
−0.427*
Grain yield
NAE
0.987**
c
RW, X^2 = 8.189, P = 0.146, GFI = 0.911, RMSEA = 0.188
Fertilization (CU:1, BBU:2)
0.344
0.377
pH
SOC
0.578*
POXC
Soil nutrients
0.461*
Grain yield
NAE
0.943**